



Comparison of Time Series Forecasting Techniques Applied for Water Quality Prediction in Southwest Iran

ARTICLE INFO

Article Type

Original Research

Authors

Sakizadeh M.*¹ PhD

How to cite this article

Sakizadeh M. Comparison of Time Series Forecasting Techniques Applied for Water Quality Prediction in Southwest Iran. ECOPERSIA. 2020;8(4):199-208.

ABSTRACT

Aims The main objective of the current study was to assess the efficiency of four-time series prediction methods to forecast the values of total dissolved solids (TDS) using a time series of over sixteen years.

Materials & Methods The applied methods comprised of autoregressive integrated moving average (ARIMA) as the most traditional method, two neural network based techniques including multilayer perceptron (MLP) along with extreme learning machines (ELM) and a novel approach known as temporal hierarchies (TH) which was applied for the first time in water resources and water quality researches.

Findings It was found that with respect to the forecasting accuracy, the MLP outperforms the ARIMA model for the training series where the MAPE (%) and MASE (mg/l) were reduced from 5.109 to 3.146 and 0.553 to 0.323, respectively. On the other hand, the forecasting accuracy of ELM was lower than that of MLP however the respective out-of-sample generalization ability of this model was higher with MAPE and MASE values of 6.526 and 0.683.

Conclusion Meanwhile, it was concluded that temporal hierarchies gave the best results for the test part of time series. The main shortcoming of neural network based approaches was their reduced out-of-sample prediction due to overfitting. Based on the results, TH is a viable alternative for conventional time series forecasting techniques.

Keywords Arima; Neural Network; Temporal Hierarchies; Time Series; Water Quality

¹Environmental Sciences Department, Shahid Rajaei Teacher Training University, Tehran, Iran

*Correspondence

Address: Environmental Sciences Department, Shahid Rajaei Teacher Training University, Tehran, Iran.
Phone: +98 (21) 22970060
Fax: +98 (21) 22970033
msakizadeh@gmail.com

Article History

Received: July 28, 2019

Accepted: December 24, 2019

ePublished: September 22, 2020

CITATION LINKS

[1] A novel hybrid water quality time series prediction method ... [2] New formulation of fuzzy comprehensive evaluation ... [3] Application of several data-driven techniques for ... [4] Efficient implementation of inverse approach for ... [5] Hydrological drought forecasting using ARIMA ... [6] Improving forecasting accuracy of annual runoff ... [7] Copula-based Markov process for forecasting and ... [8] Multi-step ahead modelling of river water quality ... [9] Spatial distribution of nitrate health risk associated ... [10] Water quality prediction based on recurrent neural network ... [11] Groundwater resources and quality in northeastern ... [12] Regional hydrochemical study on salinization ... [13] Time series analysis of aerosol optical depth over New ... [14] Application of several data-driven techniques for ... [15] A stochastic modelling technique for groundwater ... [16] A hybrid neural network and ARIMA model for water ... [17] Reservoir inflow forecasting using ensemble ... [18] Neural network ensemble operators for time series ... [19] Neural networks and learning ... [20] Forecasting with temporal ... [21] Prediction of soil organic carbon at the European ... [22] Another look at measures of forecast ... [23] Pollution profiles and health risk assessment of VOCs ... [24] Water quality data: Analysis and ... [25] Geochemistry of the Karkheh River sediments ... [26] Evaluation of river-aquifer interaction in the north ... [27] Influence of Sungun copper mine on groundwater ... [28] The analysis of time series: an ... [29] Model selection techniques for the frequency analysis ... [30] A new metric of absolute percentage error ... [31] Forecasting methods and ... [32] Dropout: A simple way to prevent neural networks ...

Introduction

Deterioration of water quality is a widespread phenomenon in developing countries. With the advent of advanced and efficient on-line systems for analysis of water quality, application of time series analysis techniques has increased in environmental researches in order to provide early predictions about future trends in water quality, as well as facilitate decision making for managers [1]. Among different methods, auto-regressive (AR), moving average (MA), hybrid of the latest two approaches known as ARMA, along with auto-regressive integrated moving average (ARIMA) were the most conventional techniques for time series analysis in water resources and water quality studies [2, 3]. However even though, following successful usage of neural network as a machine learning approach in different fields of studies, this method was also popular in time series prediction of water quality and quantity [4, 5].

There have been multiple applications of time series forecasting in water quality researches. For example, a hybrid method of heuristic Gaussian cloud transformation and fuzzy time series was applied by Deng *et al.* [1] to predict the time series of dissolved oxygen (DO), chemical oxygen demand (COD), water temperature, and electrical conductivity (EC) in China. A combined method of empirical mode decomposition (EEMD), as well as ARIMA, was utilized by Wang *et al.* [6] in order to improve the forecasting accuracy of traditional ARIMA technique for forecasting annual runoff time series [6]. Arya and Zhang [7] applied bivariate and D-Vine copula for first-order and higher-order Markov processes in order to model water quality time series. The best performed Markov process was then utilized for risk assessment with respect to the Value-at-Risk (VaR) criterion at Snohomish and Chattahoochee River Watersheds, USA. It was concluded that these techniques are able to properly model dissolve oxygen (DO), temperature and nitrate time series with high accuracy [7]. More recent studies, [8] compared the performance of artificial intelligence (AI), back propagation neural network (BPNN), adaptive neuro fuzzy inference system (ANFIS), support vector machine (SVM), as well as ARIMA for forecasting of dissolved oxygen in the Yamuna River, India. It was concluded that for different sampling stations considered, ANFIS

together with SVM performed better than the other models. Additionally, Fabro *et al.* [9] introduced a new model combining recurrent neural network (RNN) with improved Dempster/Shافر (D-S) evidence theory (RNNs-DS) for prediction of permanganate index, pH, total phosphorus, and dissolved oxygen from Jiuxishuichang monitoring station near Qiantang River, China. The results demonstrated that in comparison with support vector regression (SVR) and backpropagation neural network (BPNN) along with three RNN models, the new model shows higher accuracy and better stability as indicated by four performance indices.

In this context, among water quality parameters, total dissolved solids (TDS) is a representative parameter implying combined effects of inorganic and organic components, although contribution of inorganic parameters is far higher. With respect to inorganic parameters, some water quality variables such as calcium (Ca^{2+}), magnesium (Mg^{2+}), sulfate (SO_4^{2-}), sodium (Na^+), chloride (Cl^-), bicarbonate (HCO_3^-), potassium (K^+), and nitrate (NO_3^-) play a significant role. Other than the latest parameter, none of the mentioned water quality variables pose a significant risk to the health of water consumers [10].

On the other hand, high TDS values may indicate degradation of groundwater quality in areas where overexploitation is prevalent meaning that abstraction exceeds recharge and groundwater consumption is not sustainable [11]. Moreover, high levels of TDS in coastal aquifers may reflect seawater intrusion to groundwater system [12]. Therefore, in view of water management, this parameter is of paramount importance to distinguish areas of aquifer that are at risk. The main objective of the current study was to investigate the feasibility of selected time series forecasting techniques for predicting temporal changes of TDS. Meanwhile, four methods were used for this purpose including two neural network based time series forecasting approaches, ARIMA as the most applied traditional method for time series prediction along with a novel technique known as temporal hierarchies. To the best of the author's knowledge, this is the first time that the latest technique is being applied in environmental and water resources researches.

Materials and Methods

Time series forecasting

The dataset used in the current study obtained from the monthly monitoring network of Khuzestan Water and Power Authority (KWPA) and consisted of potassium (K^+), sodium (Na^+), magnesium (Mg^{2+}), calcium (Ca^{2+}), bicarbonate (HCO_3^-), sulfate (SO_4^{2-}), chloride (Cl^-), and total dissolved solids (TDS) collected between 1996 and 2012. Since TDS is representative of all other investigated water quality parameters so, it was applied for time series prediction.

For prediction purposes, the respective time series was separated into training and test set to have an out-of-sample data to investigate the generalization ability of each method of interest. The series between 1996 and 2007 were utilized for training and the last five years were retained as the test set to be consistent with the approach followed by Taneja *et al.* [13] and Shirmohammadi *et al.* [14]. Since the time series of TDS was positively skewed, the TDS data were log-transformed in order to comply with the normality requirement. In addition, the stationary requirement was fulfilled by differencing of the time series. Three different modeling algorithms were used for time series prediction including autoregressive integrated moving average (ARIMA), ensemble of neural networks (NN) which consisted of extreme learning machine (ELM) and multilayer perceptron (MLP) plus a novel technique known as temporal hierarchies (TH).

Autoregressive integrated moving average (ARIMA) models have been used widely for time series predictions [15]. The main shortcoming of this method is that it cannot handle nonlinear relationships while both linear and nonlinear patterns are dominant in a time series data [16]. In ARIMA modeling technique, the predicted values are assumed to be a linear function of the preceding observed values plus random errors.

(1)

ARIMA (p, d, q)

Where the non-seasonal part of the model is specified as (p, d, q). In the above-mentioned equation, the order of non-seasonal autocorrelation and regular differencing are represented by p and d whereas the order of non-seasonal moving average (MA) is defined by q, respectively.

On the contrary, it has been known from previous researches that forecasting accuracy of

ensemble of neural networks is higher than single neural networks since they are less sensitive to poor initial values and are more efficient, accordingly [17]. The limitation of ARIMA models for prediction of linear time series has encouraged some of the researchers to apply neural networks (NNs) for time series prediction since they have high efficiency for both linear and nonlinear relationships [18]. In this context, the functional form of prediction by multilayer perceptron can be defined as:

(2)

$$\hat{y}_{t+1} = \beta_0 + \sum_{h=1}^H \beta_h \phi(\gamma_{0i} + \sum_{i=1}^I \gamma_{hi} p_i)$$

The forecasts (\hat{y}_{t+1}) are predicted values at time t+1 from the lagged observations (e.g. preceding time series values). In this respect, the network weights are denoted by $\omega = (\beta, \gamma)$ where $\beta = [\beta_1, \dots, \beta_H]$ and $\gamma = [\gamma_{11}, \dots, \gamma_{HI}]$ for the output and hidden layers, while the associated bias for the respective layers are represented by β_0 and γ_{0i} . On the contrary, H , $\phi(\cdot)$ and p_i are in turn the number of hidden nodes, non-linear transfer function and number of inputs. By comparing the output to the observed time series, the values of neural network weights and biases are updated iteratively such that the error is minimized. Meanwhile, each multilayer perceptron was trained 20 times with different random initializations (starting weights and biases) to avoid trapping in local minima of the error surface [19]. Since minor changes in the starting weights can result in different estimates, an ensemble of all neural networks was used to assess the uncertainty in the results. Multiple ensemble methods such as mean and median have been suggested, however, following the recommendation made by Kourentzes *et al.* [18], the mode was applied since it is insensitive to outliers. The optimal number of hidden nodes was found by assigning 20% of randomly selected data as validation part and finding the minimum mean squared error of the model for the different numbers of hidden nodes varying between 1 and 20. An alternative to ensembling in the neural network is the extreme learning machine (ELM) algorithm. The main distinguishing feature of this method compared to MLP is that there is no need to tune the hidden layer but the output weights are subsequently resolved using the least squares method.

On the contrary, in the temporal hierarchies (TH) algorithm [20], all possible temporal aggregations of a time series are computed resulting in an integer number of observations per year. For instance, the monthly time series data is aggregated to 2-monthly, quarterly, 4-monthly, biannual and annual time series. These time series are regarded as forecast followed by their reconciliation using the hierarchical reconciliation algorithm. It has been claimed that this method has higher accuracy compared to that of conventional methods and the forecasting ability of this approach is especially higher for time series with long seasonal periods. There have so far been no studies using this approach for time series prediction of water quality.

Performance analysis of forecasting models

Six error metrics were utilized to assess the performance of models. The performance criteria consisted of mean error (ME), mean absolute error [21], root mean squared error (RMSE), mean percentage error (MPE), mean absolute percentage error (MAPE), and mean absolute scaled error (MASE) according to the following equations:

$$ME = \frac{1}{n} \sum_{t=1}^n (X_t - \hat{X}_t) \tag{3}$$

$$MAE = \frac{1}{n} \sum_{t=1}^n |X_t - \hat{X}_t| \tag{4}$$

$$RMSE = \sqrt{\frac{1}{n} \sum_{t=1}^n (X_t - \hat{X}_t)^2} \tag{5}$$

$$MPE = \frac{1}{n} \sum_{t=1}^n \left(\frac{X_t - \hat{X}_t}{X_t} \right) \tag{6}$$

$$MAPE = \frac{100}{n} \sum_{t=1}^n \left| \frac{X_t - \hat{X}_t}{X_t} \right| \tag{7}$$

$$q_t = \frac{X_t - \hat{X}_t}{\frac{1}{n-1} \sum_{t=2}^n |X_t - X_{t-1}|} \tag{8}$$

$$MASE = mean(|q_t|)$$

(9)

Where X_t and \hat{X}_t are the observed and estimated values in time series, respectively. The best models are those for which the MAPE is lower than 10% that are regarded as potentially very good while the models for which MAPE is above 30% are deemed to be potentially inaccurate. In addition, one of the advantages of MASE is that it is not dependent on the scale of original data in time series [22].

Model selection in time series analysis

In time series analysis, Akaike’s information criterion [23] is often used for model selection however, it should not be used as the sole criterion for this purpose since there are some other criteria such as Akaike’s bias-corrected information criterion (AICc) and Bayesian information criterion (BIC). In model selection, a model with the smallest AIC is usually preferable. The modified version of AIC (e.g. AICc) and BIC have been proposed since for autoregressive models AR (p), AIC is likely to overestimate p while AICc and BIC contain a penalty parameter to avoid over-fitting. Like that of AIC, a model with minimum BIC is preferable. As a whole, in large samples, BIC performs better while for that of smaller samples, where the number of parameters is large, AICc outperforms that of BIC. Thus, despite the popularity of original AIC for model selection, especially in time series analysis, some experts prefer AICc and BIC.

Findings and Discussion

Groundwater quality

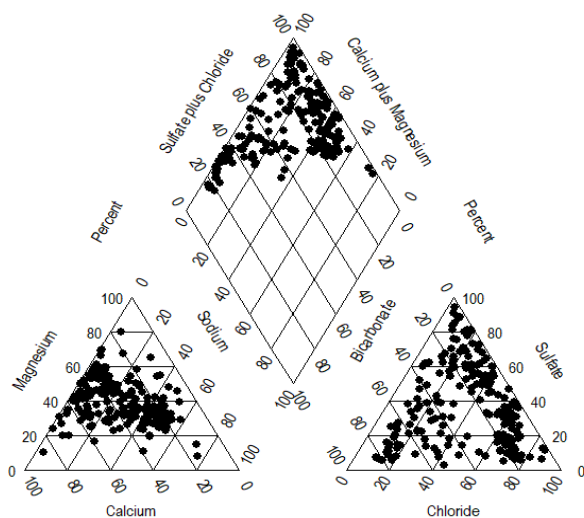
Quality assurance checks balancing the anion/cation constituents were inconclusive due to presence of nitrates (which was not measured) arising from intensive agricultural activity in the region. Assessment of ionic ratios [24] was also applied and the results produced in Table 1. The results indicate that all of the ionic or parametric ratios are within the suggested ranges. The higher values of Mg^{2+} compared to that of Ca^{2+} might be attributed to the outcrops of ultramafic rocks in the northern part of the study area resulting in a $Mg^{2+} > Ca^{2+}$ in some samples [24, 25]. The data used are therefore of reasonable quality and appropriate to be used for this study.

Table 1) Summary of reliability checks for water quality parameters*

Ionic or parametric ratios	Value			Reference
	1 st Qu.	Median	3 rd Qu.	
TDS/EC	0.639	0.663	0.735	0.55-0.76
Na ⁺ /K ⁺	33.161	89.182	192.268	Na ⁺ >>K ⁺
Ca ²⁺ /Mg ²⁺	0.662	0.849	1.227	Ca ²⁺ ≥Mg ²⁺
Na ⁺ /Cl ⁻	1.384	1.544	1.945	Na ⁺ ≥Cl ⁻
Ca ²⁺ /SO ₄ ²⁻	1.716	2.669	5.173	Ca ²⁺ ≥SO ₄ ²⁻

*Other than TDS and EC for which units of mg/l and μS/cm have been used, the scale of all other major ions is meq/l.

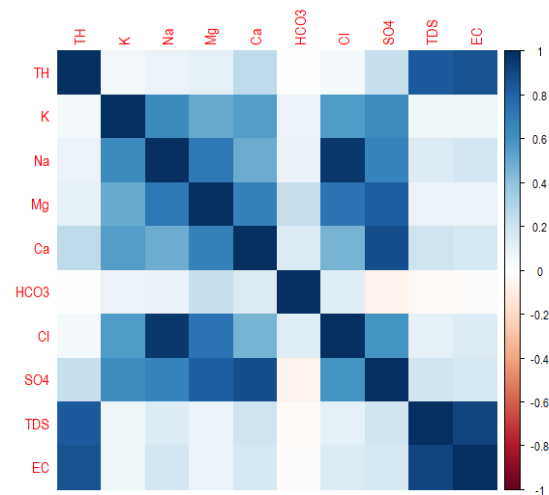
The geology within the study area is characterized by Bakhtiari conglomerate and Aghajari formations followed by outcrops of the Lahbari member and quaternary alluvial sediments in the northwestern part of the region [26]. The lithology of the latter two formations consists mainly of gypsum which contributes significantly to the ionic content of the groundwater through water-rock interaction. Diagram 1 presents a piper diagram. Referring to the piper diagram (Diagram 1), the groundwater quality in the studied station belongs to calcium sulfate waters since the majority of samples are located in the top quadrat of the diamond.

**Diagram 1)** Representation of chemistry of groundwater sample through piper diagram

Gypsum is the most abundant calcium sulfate mineral that is created under sedimentary conditions. Besides, there are small quantities of calcium bicarbonate and sodium chloride waters based on the results of the piper diagram however the contribution of these water types is far less important than calcium sulfate. As mentioned by Hounslow [24], unless otherwise Ca²⁺ is removed by precipitation or ion-exchange, in regions where Ca²⁺ emanates from

gypsum or anhydrite, the concentrations of Ca²⁺ are higher than that of SO₄²⁻. So, with respect to the results of Table 1, the detection of Ca²⁺ can be attributed to the dominance of gypsum.

The small levels of sodium chloride may be attributed to seawater encroachment into the aquifer in ancient times, due to the proximity of the study area to the Persian Gulf. The correlation heatmap in Figure 1 provides corroborating information about the sources of anions and cations and relationship with other quality parameters such as TDS, total hardness (TH), and electrical conductivity (EC). The high correlation coefficient between TDS, EC, and TH indicates that Ca²⁺ and Mg²⁺ are the main constituents of TDS [27]. The other fact that can be deduced from this panel is the high correlation between Ca²⁺ and SO₄²⁻ which is in agreement with the results of piper diagram. Moreover, the high correlation between Na⁺ and Cl⁻ may indicate the salinization of groundwater in recent years.

**Figure 1)** Correlation heatmap of groundwater quality parameters

Time series prediction

The observed time series of TDS next to the results of time series decomposition including trend, seasonal, and random components have been illustrated in Diagram 2.

It can be concluded that after accounting for the seasonal and random components, the overall trend of TDS is a gradual decrease from about 2000mg/l to roughly 1000mg/l between 1996 and 1997. Since then, the TDS level was approximately stable by 1999 but it started to increase steadily to more than 50000mg/l in 2002 however it slumped suddenly to less than

1000mg/l where it remained at this level by 2012. The most influential components are trend, followed by seasonal and random parts. The strong seasonal component reflects the impacts of precipitation on dissolution of minerals from geological formations that repeated seasonally and increased during rainy seasons. The strongest random component was coincided with the peak of trend component implying that this sudden rise may be due to error.

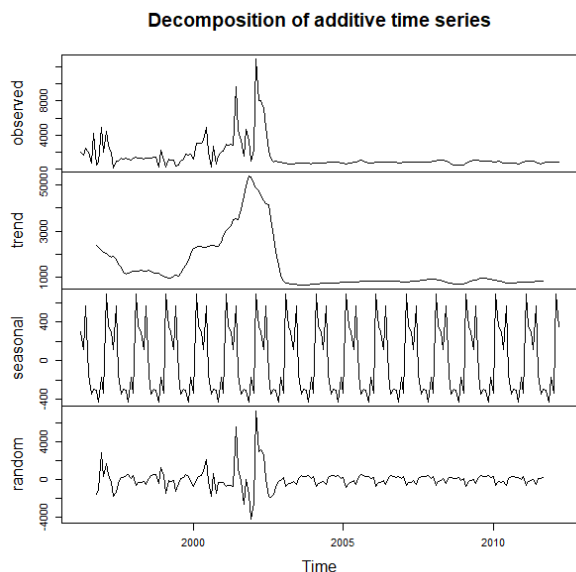


Diagram 2) Original versus decomposed components of TDS time series

One of the requirements of prediction with autoregressive integrated moving average (ARIMA) models is that the time series should be stationary, i.e., there is no systematic change in mean and variance of the time series [28]. In practice, differencing is usually performed in order to convert a non-stationary time series to satisfy the stationary requirement. The autocorrelation of the TDS time series next to that of first, second, and third difference autocorrelations are shown in Diagram 3.

The existence of a trend is noticeable in the original series as the autocorrelation function (ACF) versus lag does not decay to zero and the difference from zero for the first, second, and third difference series is small, according to the ACF. Hence, from parsimony considerations of Laio *et al.* [29], the first difference was selected. Following a trial and error optimization procedure, the final selected model was ARIMA (0, 1, 1). The Akaike's bias-corrected information criterion and Bayesian information

criterion (BIC) for this model were 23.52 and 29.18, respectively [23]. In addition, the associated values of mean error or ME (mg/l), root mean squared error or RMSE (mg/l), mean absolute error or MAE (mg/l), mean percentage error or MPE (%), mean absolute percentage error or MAPE (%), and mean absolute scaled error or MASE (mg/l) for the training set were -0.007, 0.259, 0.154, -0.836, 5.109, and 0.553, whereas for the test set they were 0.000, 0.089, 0.068, -0.085, 2.399, and 0.246, respectively (Table 2).

The best unbiased method for time series model selection is to use a hold-out sample which is not exposed to the model of interest during training. In this context, among the respective performance criteria, MAPE is the most popular and it is a scale-independent index, although some investigators advise caution because it yields infinite values for zero or close-to-zero [30, 31]. On the other hand, MASE has been claimed to be the best available scale for this purpose and was adopted for the present study [24].

For forecasting with MLP, the optimized NN was trained 20 times to produce an ensemble forecast containing a single hidden layer with 17 hidden nodes that were obtained using a trial and error procedure. With respect to the forecasting accuracy of this modeling technique, it should be noted that this model outperforms the ARIMA model for the training series where the MAPE (%) and MASE (mg/l) are reduced from 5.109 to 3.146 and from 0.553 to 0.323, respectively (Table 2). In spite of this, the performance of this model related to all of the other criteria was worse than that of ARIMA for the test set implying that the model has over-fitted the training data. This is a prevalent problem in modeling with NN and originates from a limited number of training data so the network fits the sampling noise instead of the true relationship between input and output [32]. For ELM, an optimized NN with 100 hidden nodes was created. Although 100 hidden nodes may seem to be a large number, however as emphasized by Kourentzes *et al.* [20], the lasso algorithm used for estimation of weights is a shrinkage estimator that has the capability to eliminate most of the connections. The forecasting accuracy of ELM is lower than that of MLP where the values of MAPE and MASE increased to 4.705% and 0.487mg/l, respectively. Nonetheless, it is clear that the over-fitting problem persists for this model

which may result in poor generalization ability for unseen data. The respective values of MAPE and MASE are significantly lower than MLP model though.

The final model used for time series prediction is a novel technique known as temporal hierarchies (TH) [20]. The results show that TH is the best performing model with MAPE (%) and MASE (mg/l) for the training set decreasing to 3.428 and 0.381 from 4.705 and 0.487 when compared to the ELM. Despite the fact that MLP outperformed in view of the training part however the out-of-sample forecasting ability of TH was far better and of the same order of magnitude as ARIMA model. In order to consider the performance of these models graphically, the predicted versus observed time series were depicted for the test part (Diagram 4). Considering the results, a continuous increase and decrease were forecasted by MLP and ELM time series forecasting models whereas the predicted values by ARIMA implied no change

over the following years (e.g. a horizontal line). The only model by which the fluctuations of the test part were captured (though slightly different from actual values) was the TH model. This superior capability provides enough evidence about the outperformance of TH for the test part compared to the other applied models. In this respect, due to the combination of information contained in different aggregation levels during reconciled forecasts, the identified trends in the lower aggregation levels positively contribute toward the highest level (e.g. annual level), therefore the predictions are more accurate in this approach [20]. Besides its higher forecasting accuracy, one of the advantages of TH compared to conventional methods is the reduction of uncertainties at each individual level since different temporal information is covered by each time series. Their aggregation results are therefore more robust with less variability in addition to having an improved signal to noise level [20].

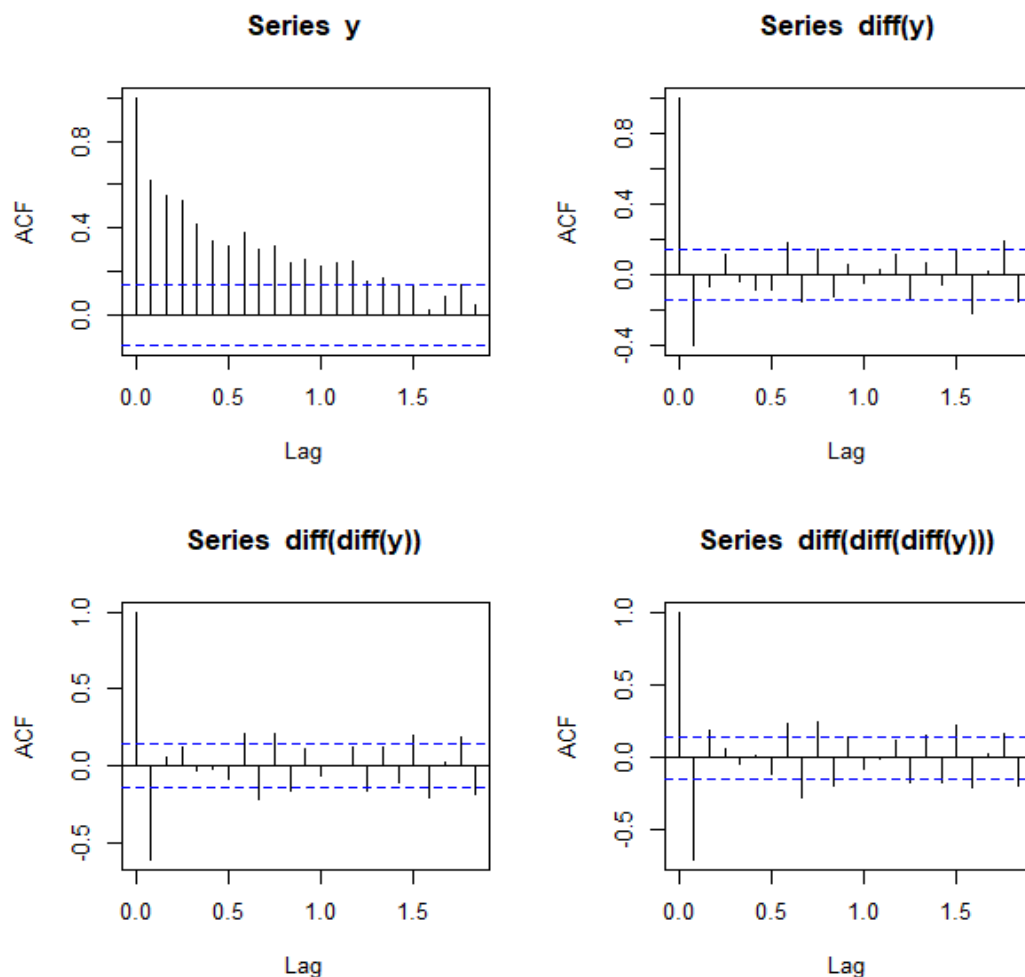


Diagram 3) Autocorrelation function (ACF) of original time series versus the first, second, and third difference series

Table 2) Time series prediction by different algorithms

Method	Training set						Test set					
	ME	RMSE	MAE	MPE	MAPE	MASE	ME	RMSE	MAE	MPE	MAPE	MASE
ARIMA*	-0.007	0.259	0.154	-0.836	5.109	0.553	0.000	0.089	0.068	-0.085	2.399	0.246
MLP**	-0.005	0.168	0.098	-0.161	3.146	0.323	0.429	0.514	0.430	14.703	14.727	1.541
ELM***	0.000	0.277	0.148	-0.027	4.705	0.487	0.017	0.217	0.190	5.787	6.526	0.683
TH****	0.000	0.152	0.106	-0.334	3.428	0.381	-0.069	0.129	0.095	-2.496	3.367	0.342

*: Autoregressive integrated moving average; **: Multilayer perceptron; ***: Extreme learning machines; ****: Temporal hierarchies

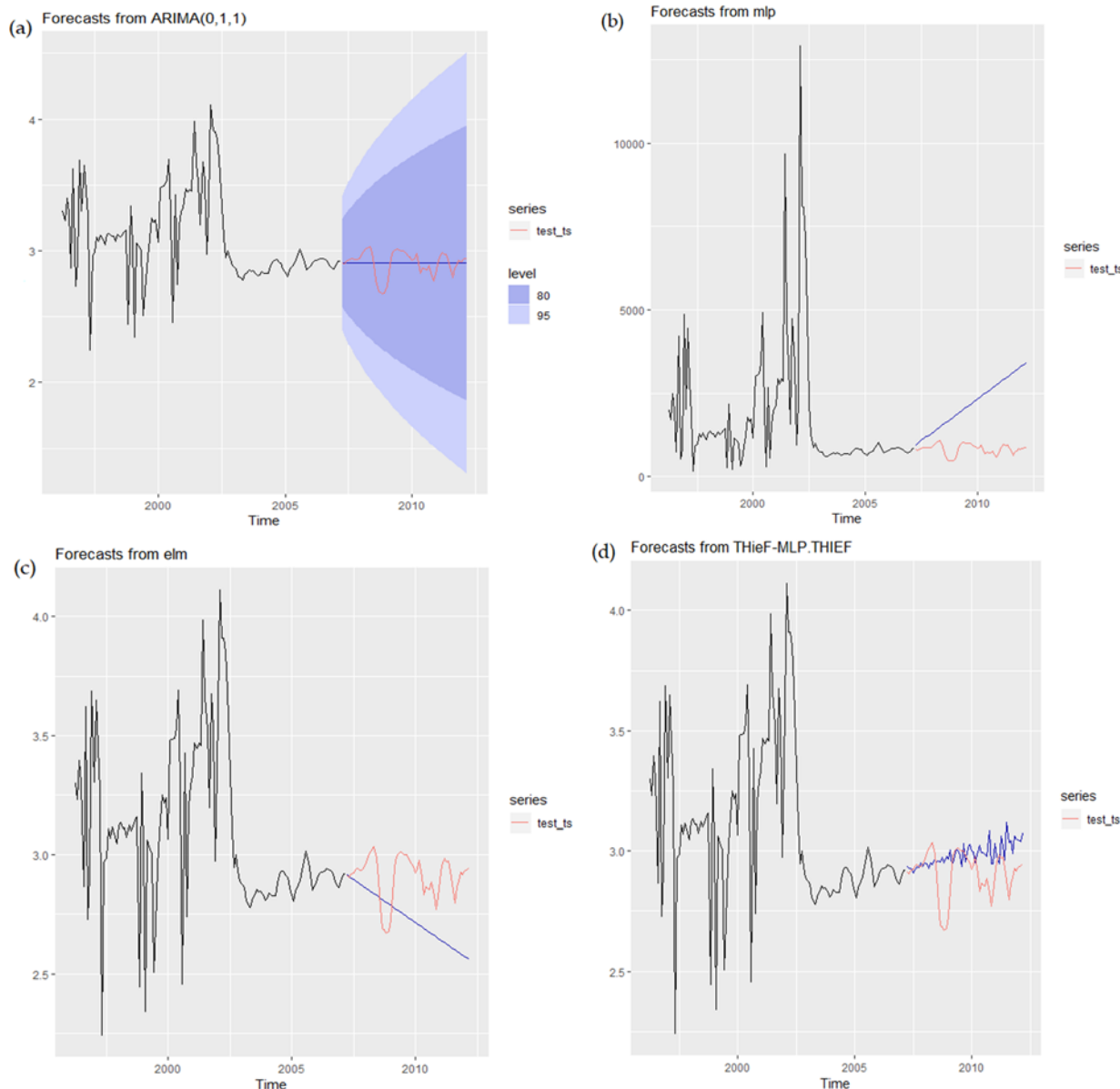


Diagram 4) Predicted time series for the test part (test_ts) using ARIMA (a), MLP (b), ELM (c), and TH (d) models in logarithmic scale

Conclusion

The ionic ratios of the groundwater anion/cation constituents indicated the impact of ultramafic rocks on the quality of groundwater exhibited by higher values of Mg²⁺ compared to that of Ca²⁺. Additionally, piper diagram proved the fact that the groundwater quality in the studied station belongs to calcium

sulfate waters. Moreover, the identified elevated levels of Ca²⁺ in some parts of the aquifer can be ascribed to the dominance of gypsum.

In the present study, the out-of-sample forecasting ability of the temporal hierarchies (TH) was superior to multilayer perceptron (MLP) however of the same order of magnitude as autoregressive integrated moving average

(ARIMA) model. With respect to the graphical comparison of the forecasted models for the test set, the only model that could capture the fluctuations of test part was the TH. It seems as if one of the main reasons for the better performance of TH compared to the other investigated models is the combination of information contained in different aggregation levels during reconciled forecasts.

Nevertheless, the major disadvantage of NNs compared to ARIMA and TH according to the findings of this study is the problem of overfitting resulting in low generalization ability (out-of-sample prediction). This study is the first application of the TH algorithm in water quality predictions and is recommended for future studies, given the positive results.

Acknowledgements: The aid of Khuzestan Water and Power Authority to execution of the current study is greatly appreciated. The data set used in this study is freely available and can be obtained upon request from the corresponding author.

Ethical Permission: There is not any ethical issue associated with this submission.

Conflicts of Interests: The authors state that there is no conflict of interests.

Authors Contribution: Sakizadeh M. Introduction author/Methodologist/Original researcher/Statistical analyst/Discussion author (100%)

Funding/Supports: The case was not declared by the authors.

References

- 1- Deng W, Wang G, Zhang X. A novel hybrid water quality time series prediction method based on cloud model and fuzzy forecasting. *Chemom Intell Lab Syst.* 2015;149(Part A):39-49.
- 2- Bahar Gogani M, Douzbakhshan M, Shayesteh K, Ildoromi AR. New formulation of fuzzy comprehensive evaluation model in groundwater resources carrying capacity analysis. *ECOPERSIA.* 2018;6(2):79-89.
- 3- Vafakhah M, Janizadeh S, Khosrobeigi Bozchaloei S. Application of several data-driven techniques for rainfall-runoff modeling. *ECOPERSIA.* 2014;2(1):455-69.
- 4- Liang SY, Phoon KK, Pasha MF, Doan CD. Efficient implementation of inverse approach for forecasting hydrological time series using micro GA. *J Hydroinform.* 2005;7(3):151-63.
- 5- Bazrafshan O, Salajegheh A, Bazrafshan J, Mahdavi M, Fatehi Maraj A. Hydrological drought forecasting using ARIMA models (case study: Karkheh Basin). *ECOPERSIA.* 2015;3(3):1099-117.
- 6- Wang WC, Chau KW, Xu DM, Chen XY. Improving forecasting accuracy of annual runoff time series using ARIMA based on EEMD decomposition. *Water Resour Manag.* 2015;29(8):2655-75.
- 7- Arya FK, Zhang L. Copula-based Markov process for

forecasting and analyzing risk of water quality time series. *J Hydrol Eng.* 2017;22(6):04017005.

8- Elkiran G, Nourani V, Abba SI. Multi-step ahead modelling of river water quality parameters using ensemble artificial intelligence-based approach. *J Hydrol.* 2019;577:123962.

9- Fabro AY, Ávila JG, Alberich MV, Sansores SA, Camargo-Valero MA. Spatial distribution of nitrate health risk associated with groundwater use as drinking water in Merida, Mexico. *Appl Geogr.* 2015;65:49-57.

10- Li L, Jiang P, Xu H, Lin G, Guo D, Wu H. Water quality prediction based on recurrent neural network and improved evidence theory: A case study of Qiantang River, China. *Environ Sci Pollut Res.* 2019;26(19):19879-96.

11- Dottridge J, Jaber NA. Groundwater resources and quality in northeastern Jordan: Safe yield and sustainability. *Appl Geogr.* 1999;19(4):313-23.

12- Park SC, Yun ST, Chae GT, Yoo IS, Shin KS, Heo CH, et al. Regional hydrochemical study on salinization of coastal aquifers, western coastal area of South Korea. *J Hydrol.* 2005;313(3-4):182-94.

13- Taneja K, Ahmad Sh, Ahmad K, Attri SD. Time series analysis of aerosol optical depth over New Delhi using Box-Jenkins ARIMA modeling approach. *Atmos Pollut Res.* 2016;7(4):585-96.

14- Shirmohammadi B, Vafakhah M, Moosavi V, Moghaddamnia A. Application of several data-driven techniques for predicting groundwater level. *Water Resour Manag.* 2013;27(2):419-32.

15- Mirzavand M, Ghazavi R. A stochastic modelling technique for groundwater level forecasting in an arid environment using time series methods. *Water Resour Manag.* 2015;29(4):1315-28.

16- Faruk DÖ. A hybrid neural network and ARIMA model for water quality time series prediction. *Eng Appl Artif Intell.* 2010;23(4):586-94.

17- Kumar S, Tiwari MK, Chatterjee Ch, Mishra A. Reservoir inflow forecasting using ensemble models based on neural networks, wavelet analysis and bootstrap method. *Water Resour Manag.* 2015;29(13):4863-83.

18- Kourentzes N, Barrow DK, Crone SF. Neural network ensemble operators for time series forecasting. *Expert Syst Appl.* 2014;41(9):4235-44.

19- Haykin SS, Haykin SS, Haykin SS, Haykin SS. *Neural networks and learning machines.* 3rd Edition. Upper Saddle River: Prentice Hall; 2009.

20- Athanasopoulos G, Hyndman RJ, Kourentzes N, Petropoulos F. Forecasting with temporal hierarchies. *Eur J Oper Res.* 2017;262(1):60-74.

21- Stevens A, Nocita M, Tóth G, Montanarella L, Van Wesemael B. Prediction of soil organic carbon at the European scale by visible and near infrared reflectance spectroscopy. *PLoS One.* 2013;8(6):e66409.

22- Hyndman RJ, Koehler AB. Another look at measures of forecast accuracy. *Int J Forecast.* 2006;22(4):679-88.

23- An T, Huang Y, Li G, He Z, Chen J, Zhang Ch. Pollution profiles and health risk assessment of VOCs emitted during e-waste dismantling processes associated with different dismantling methods. *Environ Int.* 2014;73:186-94.

24- Hounslow A. *Water quality data: Analysis and interpretation.* Boca Raton: CRC Press; 2018.

25- Zarasvandi A, Mirzaee S. Geochemistry of the Karkheh River sediments, Khuzestan Province, Iran: Evidences for natural contamination. *Res J Appl Sci.* 2009;4(1):35-40.

26- Chitsazan M, Faryabi M, Zarrasvandi AR. Evaluation of

Comparison of Time Series Forecasting Techniques Applied ...

river-aquifer interaction in the north part of Dezful-Andimeshk district, SW of Iran. Arab J Geosci. 2015;8(9):7177-89.

27- Nasrabadi T, Nabi Bidhendi GR, Karbassi AR, Hoveidi H, Nasrabadi I, Pezeshk H, et al. Influence of Sungun copper mine on groundwater quality, NW Iran. Environ Geol. 2009;58(4):693-700.

28- Chatfield Ch. The analysis of time series: an introduction. Boca Raton: CRC Press; 2016.

29- Laio F, Di Baldassarre G, Montanari A. Model selection techniques for the frequency analysis of hydrological

extremes. Water Resour Res. 2009;45(7):W07416.

30- Kim S, Kim H. A new metric of absolute percentage error for intermittent demand forecasts. Int J Forecast. 2016;32(3):669-79.

31- Makridakis S, Wheelwright SC, Hyndman RJ. Forecasting methods and applications. Hoboken: John Wiley & Sons; 2008.

32- Srivastava N, Hinton G, Krizhevsky A, Sutskever I, Salakhutdinov R. Dropout: A simple way to prevent neural networks from overfitting. J Mach Learn Res. 2014;15(1):1929-58.